NANO LETTERS

2008
Vol. 8, No. 8
2219-2223

Expedient Vapor Probing of Organic Amines Using Fluorescent Nanofibers Fabricated from an n-Type Organic Semiconductor

Yanke Che,[†] Xiaomei Yang,[†] Stephen Loser,[‡] and Ling Zang*,[†]

Department of Chemistry and Biochemistry, Southern Illinois University, Carbondale, Illinois 62901

Received March 16, 2008; Revised Manuscript Received May 24, 2008

ABSTRACT

A new type of fluorescence sensory material with high sensitivity, selectivity, and photostability has been developed for vapor probing of organic amines. The sensory material is primarily based on well-defined nanofibers fabricated from an n-type organic semiconductor molecule, *N*-(1-hexylheptyl)perylene-3,4,9,10-tetracarboxyl-3,4-anhydride-9,10-imide. Upon deposition onto a substrate, the entangled nanofibers form a meshlike, highly porous film, which enables expedient diffusion of gaseous analyte molecules within the film matrix, leading to milliseconds response for the vapor sensing.

Development of sensors or probes that can be used to detect the trace vapor of organic amines represents one of the active research fields in chemistry and materials science,[1–5] particularly those related to the emerging nanoscience and nanotechnology.[6–10] Volatile amines have been heavily used in various areas ranging from chemical to pharmaceutical and to food industries.[2] Some of the amines, like hydrazine, have also been used in the military as fuel additives in rocket and fighter jet propulsion systems. Detecting these amines in high sensitivity not only is critical to air pollution monitoring and control but also may provide expedient ways for quality control of food and even medical diagnosis of certain types of disease, for example, uremia and lung cancer, for which biogenic amines released are usually used as biomarkers.[11,12] Although much success has been achieved for detection of amines in solutions using various types of sensors,[13–15] the vapor-based detection of gaseous amines still remains challenging, mainly due to the limited availability of sensory materials that enable vapor detection with both high sensitivity and selectivity.[16]

Fluorescent sensing and probing based on organic sensory materials represents a unique class of detection techniques that usually provide a simple, expedient way for chemical detection and analysis. However, there are not many organic materials available that are sufficiently fluorescent in solid state[17–19] and suited to be used as sensory materials for vapor detection,[16] although these materials may be strongly fluorescent in molecular state in solutions. Moreover, compared to the more common p-type (i.e., electron donating) materials, which are suited for sensing oxidative reagents like nitro-based compounds,[16,20] the availability of n-type organic materials (i.e., electron accepting, and suited for sensing reducing reagents like amines) is much more limited.[21] Herein we report on a strongly fluorescent n-type organic semiconductor material, which can be fabricated into well-defined nanofibers and employed in efficient fluorescent probing of gaseous amines.

The reported study was partially inspired by our recent successful fabrication of nanofibers from a p-type organic material and the application in sensing of nitro-based explosives.[20] The long-range exciton migration intrinsic to the one-dimensional well-organized molecular arrangement within the nanofiber enables amplified fluorescence quenching by the surface adsorbed analytes (quencher molecules). Taking advantage of such amplified fluorescence quenching intrinsic to nanofibers, we attempted to fabricate a new type of nanofibers from an n-type material that could potentially be used for effective sensing of reductive compounds, such as organic amines, through electron-transfer-based fluorescence quenching. The building block molecule (**1**) employed for the nanofibril fabrication is shown in Chart 1, which was synthesized through partial hydrolysis of hexylheptyl substituted 3,4,9,10-perylene-tetracarboxylic diimide (PTCDI) (see Supporting Information). PTCDI represents a robust class of n-type organic materials with strong photostabil-

* Corresponding author. E-mail:lzang@eng.utah.edu.
[†] Present address: Department of Materials Science and Engineering, University of Utah, 122 S. Central Campus Drive, Salt Lake City, UT 84112.
[‡] Present address: Department of Chemistry, Northwestern University, 2145 Sheridan Rd., Evanston, IL 60208.

10.1021/nl080761g CCC: $40.75
Published on Web 07/09/2008

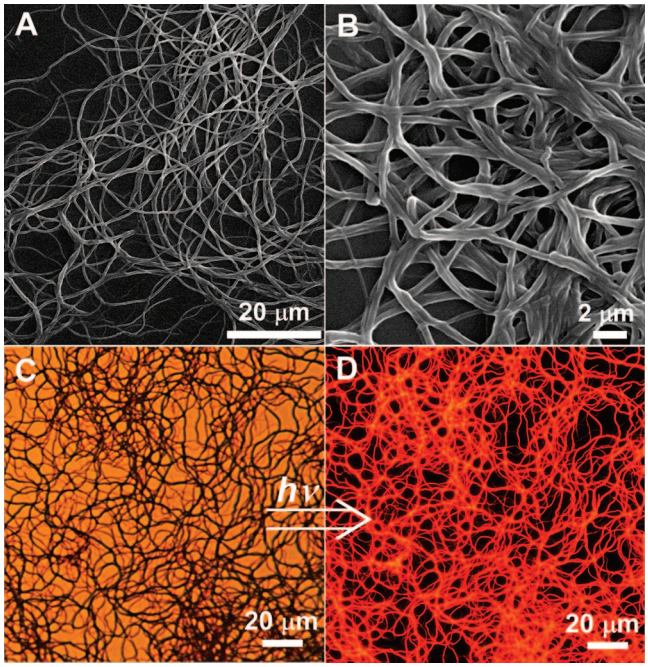

Figure 1. (A) SEM image of a nanofibril film deposited on a glass slide. (B) Zoom-in SEM image of the nanofibril film. (C, D) Bright-field and fluorescence optical microscopy image of a nanofibril film. Note: due to the diffraction effect the fiber in the optical microscopy image appears larger than the real size as measured by SEM.

Chart 1

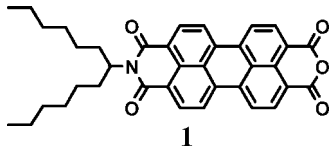

1

ity,[21–24] which is particularly desirable for being used in optical sensing or probing regarding both the performance sustainability and reproducibility.

Molecule **1** possesses a structure that provides a good balance between the molecular stacking and the fluorescence yield of the materials thus assembled.[22] The former prefers a molecular structure with minimal steric hindrance (usually referring to a small or linear side chain),[25–29] while the latter favors bulky, branched side chains that may distort the $\pi-\pi$ stacking to afford increased fluorescence (by enhancing the low-energy excitonic transition) for the molecular assembly.[16,18,29,30] Figure 1A shows the scanning electron microscopy (SEM) image of the nanofibers fabricated from **1** through a vapor-diffusion (slow solvent exchange) process as described in Figure S1. The average diameter of the nanofibers is ~350 nm as determined by zoom-in SEM imaging as shown in Figure 1B. The extended one-dimensional molecular arrangement obtained for molecule **1** is likely dominated by the $\pi-\pi$ interaction between the perylene backbones (which is sterically favored by the bare end of **1**), in cooperation with the hydrophobic interactions between the side chains in appropriate size. Such an optimal molecular arrangement is reminiscent of the one-dimensional self-assembly commonly observed for detergents, lipids, or amphiphilic peptides,[31–35] for which extended molecular

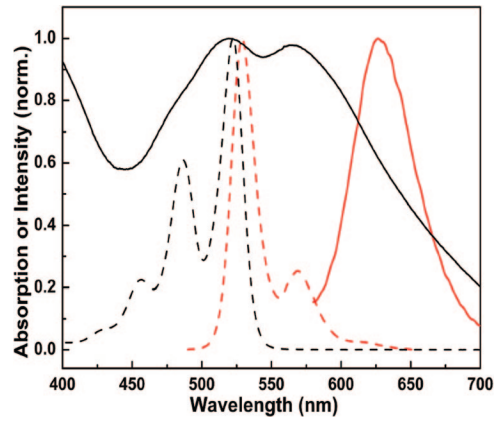

Figure 2. The absorption (black) and fluorescence (red) spectra of **1** in chloroform solution (dashed) and the nanofiber state (solid). The raised baseline for the absorption spectrum of nanofibril film is primarily due to the light scattering.

assembly can be achieved through the concerted electrostatic and hydrophobic interactions. Indeed, an asymmetric PTCDI molecule modified with two different side chains has recently been employed in a successful fabrication of millimeter long nanofibers from this laboratory.[27] It seems that one-dimensional molecular assembly of **1** is critically dependent on the size of the side chains, that is, replacing the side chain of **1** with a larger group, for example, nonyldecyl, resulted in formation of only ill-shaped molecular aggregates. The nanofibers fabricated from **1** demonstrates strong fluorescence with yield ~15% as depicted in the fluorescence microscopy images (Figure 1, panels C and D), implying a distorted molecular stacking that is usually observed for the PTCDI molecules modified with branched side chains.[18,22,29,30] The strong red fluorescence of the nanofibers can easily be observed even with the naked eye, making the nanofibers more feasible to be used in fluorescence sensing as shown in a movie clip provided in the Supporting Information.

Figure 2 shows the absorption and fluorescence spectra measured from the nanofibers deposited on glass substrate, in comparison to the spectra measured for molecule **1** dissolved in a chloroform solution. The electronic property of **1** as depicted in Figure 2 is quite similar to the parent PTCDI molecules with the HOMO−LUMO gap around 2.5 eV, consistent with the ab initio calculation results (Figure S2). The fluorescence quantum yield of **1** in solution is ~100%, the same as other PTCDI molecules. Upon assembly into the solid state, the fluorescence of individual molecules disappeared, while a new emission band formed at the longer wavelength, centered around 628 nm. Compared to the emission spectrum (0.21 eV fwhm) obtained from the ill-shaped molecular aggregate formed from the parent PTCDI molecule modified with two hexylheptyl side chains (Figure S3), the emission measured for the nanofibers of **1** exhibits a significantly narrower band, only 0.17 eV fwhm, implying the well-organized molecular assembly within the nanofibers. Consistently, a new, pronounced band was observed at the longer wavelength in the absorption spectrum of the nanofibers, which is typically characteristic of the strong $\pi-\pi$

interaction as observed in the self-assemblies of PTCDI and other planar π-conjugated molecules.[26–29,36,37] The strong $\pi-\pi$ interaction is also revealed by the characteristic enhancement of the transitions (absorptions) from ground state to the higher levels of electronic states (0−1, 0−2, and 0−3, compared to 0−0) of the component molecules. The strong $\pi-\pi$ interaction may enhance the exciton migration, which is now more confined along the long axis of the nanofiber, leading to amplification in fluorescence quenching by the surface adsorbed analytes (quenchers).

Upon fabrication from hydrophilic solvents such as alcohols, the nanofibers are expected to possess a surface predominantly consisting of the anhydride moieties, which are more hydrophilic compared to the hexylheptyl group located at the other end of the molecule. Such solvent-modulated molecule arrangement was previously employed for the self-assembly of many other amphiphilic molecules.[38–40] A surface full of anhydride moieties enables strong chemical binding or adsorption with amines through both hydrogen bonding and donor−acceptor (charge transfer) interaction. Deposition of the nanofibers onto a substrate produces a meshlike film that is primarily formed by entangled piling of the fibers and thus possesses porosity on a number of length scales (Figure 1). Such a porous film not only provides increased surface area for enhanced adsorption of gaseous molecules but also enables expedient diffusion of guest molecules across the film matrix, leading to efficient probing of the gaseous molecules with both high sensitivity and fast time response. Indeed, as shown in Figure 3A, upon exposure to the saturated vapor of aniline (880 ppm) the fluorescence of the nanofibril film was instantaneously quenched by almost 100%. Such efficient fluorescent sensing was also observed for a broad range of amines (primary, secondary, and tertiary) as listed in Table S1. The fluorescence quenching thus observed is due to a photoinduced electron transfer process as depicted in Figure S2, where the electron transfer is driven by the favorable energy difference between the HOMO of aniline and the HOMO of PTCDI (which is now one electron vacant in the excited state). The high efficiency of the fluorescence quenching is consistent with the large driving force for the photoinduced electron transfer between the excited state of molecule **1** and the amine molecules (Figure S2 and Table S1). The same photoinduced electron transfer was previously observed between the covalently linked aniline and PTCDI moiety.[41]

To explore the detection limit for some of the representative amines such as aniline and hydrazine, the same quenching process shown in Figure 3A was also examined for the diluted amine vapor (Figure S4). Figure 3B shows the fluorescence quenching efficiency ($1 - I/I_0$) of a nanofibril film measured at three different vapor pressures of aniline, 1, 10^3, and 10^4 times diluted from the saturated vapor (880 ppm) at room temperature. The quenching data are well-fitted to the Langmuir equation with an assumption that the quenching efficiency is proportional to the surface adsorption (coverage) of amines. From the fitted plot the detection limit of the nanofibril film shown in Figure 3B can be projected as low as ~200 ppt, if considering the fact that a well-

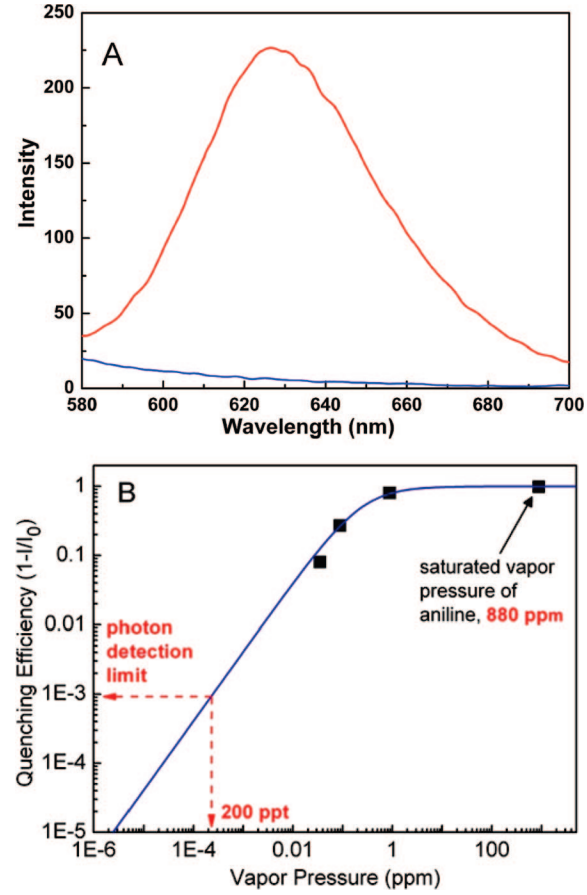

Figure 3. (A) Fluorescence spectra of a nanofibril film before (red) and after (blue) exposure to the saturated vapor of aniline (880 ppm) for 10 s. (B) Fluorescence quenching efficiency ($1 - I/I_0$) as a function of the vapor pressure of aniline: data (error ±5%) fitted with the Langmuir equation.

calibrated photodetector (e.g., PMT) can detect intensity change as small as 0.1% or below.[42] Following the same procedure the detection limit for hydrazine was estimated to be ~1 ppb.

Figure 4 shows the emission intensity of the film monitored as a function of the time after exposed to the saturated vapor of aniline (880 ppm). Fitting the intensity decay into a single exponential kinetics deduces a response time for the quenching process (defined as the decay lifetime), only 0.32 s. The fast response thus obtained for the nanofibril sensor is mainly due to the three-dimensional continuous, porous structure formed by the entangled piling of the nanofibers, which allows for expedient diffusion of the analyte molecules throughout the film matrix, thus leading to instant capture (and accumulation) of the vapor species. The fast sensing response, along with the low detection limits and the robust photostability (zero photobleaching, as shown in Figure S5) observed, makes the nanofibril film an ideal probing system in a broad range of applications, particularly for onsite amine monitoring and screening, where instant vapor detection of trace amines is usually demanded.

The nanofibril film also demonstrated high selectivity in response to organic amines, with minimal fluorescence quenching observed for other common organic reagents, such as those listed in Figure 5. For all the amines tested, more

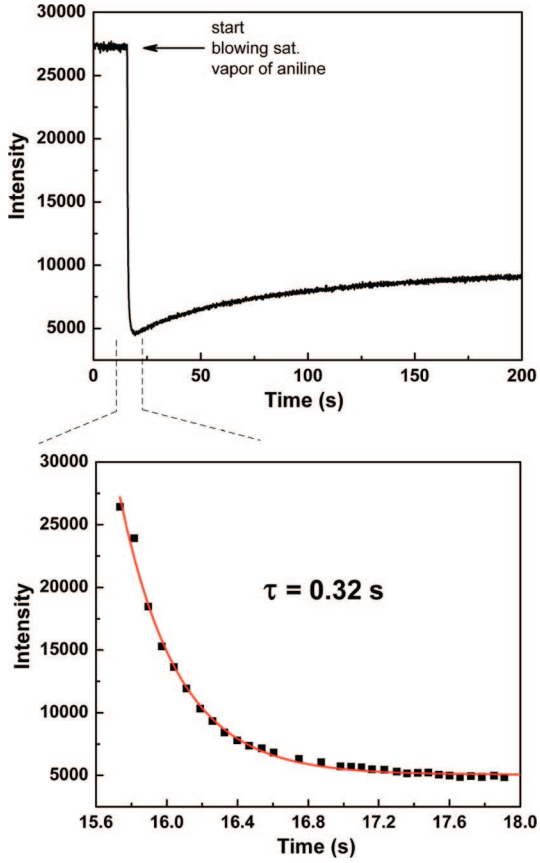

Figure 4. Time-course of fluorescence quenching of a nanofibril film upon blowing over with saturated vapor of aniline (880 ppm), indicating a response time of about 0.32 s. The intensity was monitored at 628 nm.

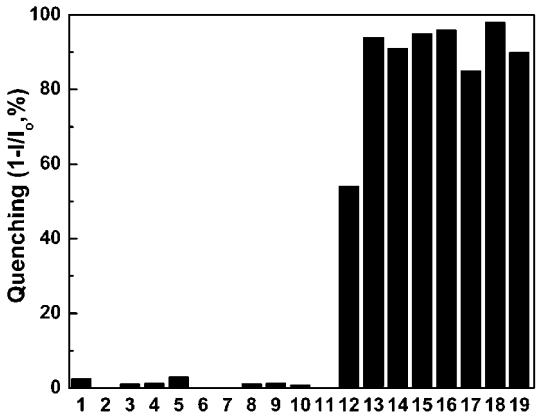

Figure 5. Fluorescence response of the nanofibril film to the saturated vapor of various organic reagents: 1, methanol; 2, acetone; 3, acetic acid; 4, THF; 5, acetonitrile; 6, chloroform; 7, toluene; 8, hexane; 9, cyclohexane; 10, nitromethane; 11, nitrobenzene; 12, phenol; 13, cyclohexylamine; 14, dibutylamine; 15, aniline; 16, butylamine (3 s); 17, triethylamine; 18, hydrazine; 19, ammonium hydroxide. Unless otherwise marked, the exposure times for the amines and all the other reagents are 10 and 15 s, respectively.

than 85% fluorescence quenching was observed for the nanofibril film upon exposure to the saturated vapor of amines, whereas all the other organic liquids and solids (except for phenol) examined as the potential background interference exhibited less than 3% fluorescence quenching under the same testing conditions (Figure 5). The significant quenching (~54%) observed with phenol is likely due to its strong reducing power, i.e., electron-donating capability. Interestingly, the fluorescence quenching observed with phenol was highly reversible as shown in Figure S6, where the fluorescence of the nanofibril film after exposure to the phenol vapor could be recovered almost 100% simply by re-exposing it to atmosphere for ~60 min (or at an elevated temperature, e.g., 60 °C, for only 5 min). The recovered film demonstrated the same quenching efficiency when used in the next cycle of the test with the phenol vapor (Figure S6). Such a reversible quenching can be used to distinguish phenol (if present) from the organic amines, which otherwise exhibited almost irreversible fluorescence quenching under the same conditions, i.e., only ~50% of the fluorescence could be restored even after heating up the film overnight. The less reversibility observed for the quenching with amines is largely due to the much more stable chemical binding between amines and the anhydride moiety of molecule 1. We consider the reported fluorescence sensor system as a single-use device, in the similar manner as a pH paper or pregnancy kit, which can be used by ordinary people without worrying about how to recover the materials after each use.

Although the fluorescence of the nanofibers cannot be recovered after exposed to the amines, the PTCDI materials (molecules) can be recovered simply by redissolving the nanofibers into chloroform, followed by appropriate purification (e.g., extraction with water) to remove the amines. The PTCDI molecules thus recovered (showing again the 100% fluorescence quantum yield) can be refabricated into the nanofibers and maintain the same sensing efficiency for amines. To this end, the PTCDI materials are recyclable, in contrast to the other irreversible sensor systems, for which the sensor materials are usually unrecyclable due to permanent chemical damage.

In conclusion, a new type of fluorescence sensory material with high sensitivity, selectivity, and photostability has been developed for vapor detection of organic amines. The sensory material is primarily based on well-defined nanofibers fabricated from an n-type organic semiconductor molecule. Upon deposition onto a substrate, these entangled nanofibers form a meshlike, highly porous film, which allows for maximal exposure to the gaseous analyte molecules, expedient diffusion of the molecules throughout the meshlike film, and increased adsorption and accumulation of the gaseous molecules within the porous matrix. Compared to the electrical sensors like those based on chemiresistors,[2,3,5] the reported fluorescent sensor system represents a class of simple, expedient technique for chemical detection and analysis. In contrast to the polymer-film-based fluorescent sensors,[1] the nanofibril-film-based sensors provide three-dimensional continuous pores (or channels) formed by the entangled piling of the nanofibers, enabling expedient diffusion of the analyte molecules throughout the film matrix, and thus fast response (milliseconds) for the sensing. The nanofibril materials, as well as the new sensing module thus developed, may open wide options to improve the detection

efficacy and find broad range of applications in health and security examination, where instant detection of trace amine is usually demanded.

Acknowledgment. This work was supported by NSF (CAREER CHE 0641353, CBET 730667) and ACS-PRF (45732-G10).

Supporting Information Available: Synthesis, nanofibril fabrication, microscopy/spectroscopy characterization, more quenching data for 10 amines, and a link to a movie clip showing the fast fluorescence quenching upon blowing with aniline vapor. This material is available free of charge via the Internet at http:// pubs.acs.org.

References

(1) Thomas, S. W., III; Swager, T. M. *Adv. Mater.* **2006**, *18* (8), 1047–1050.
(2) Gao, T.; Tillman, E. S.; Lewis, N. S. *Chem. Mater.* **2005**, *17* (11), 2904–2911.
(3) Virji, S.; Kaner, R. B.; Weiller, B. H. *Chem. Mater.* **2005**, *17* (5), 1256–1260.
(4) Reppy, M. A.; Cooper, M. E.; Smithers, J. L.; Gin, D. L. *J. Org. Chem.* **1999**, *64* (11), 4191–4195.
(5) Ellis, D. L.; Zakin, M. R.; Bernstein, L. S.; Rubner, M. F. *Anal. Chem.* **1996**, *68* (5), 817–822.
(6) Wang, X.; Wang, Z. L. *Nanoeng. Struct., Funct., Smart Mater.* **2006**, 99.
(7) Xia, Y.; Yang, P.; Sun, Y.; Wu, Y.; Mayers, B.; Gates, B.; Yin, Y.; Kim, F.; Yan, H. *Adv. Mater.* **2003**, *15* (5), 353–389.
(8) Zhang, D.; Li, C.; Liu, X.; Han, S.; Tang, T.; Zhou, C. *Appl. Phys. Lett.* **2003**, *83* (9), 1845–1847.
(9) Virji, S.; Huang, J.; Kaner, R. B.; Weiller, B. H. *Nano Lett.* **2004**, *4* (3), 491–496.
(10) Liu, H.; Kameoka, J.; Czaplewski, D. A.; Craighead, H. G. *Nano Lett.* **2004**, *4* (4), 671–675.
(11) Preti, G.; Labows, J. N.; Kostelc, J. G.; Aldinger, S.; Daniele, R. *J. Chromatogr. Biomed. Appl.* **1988**, *432*, 1.
(12) Simenhoff, M. L.; Burker, J. F.; Saukkonen, J. J.; Ordinario, A. T.; Doty, R. N. *N. Engl. J. Med.* **1977**, *297*, 132.
(13) Zhang, C.; Suslick, K. S. *J. Am. Chem. Soc.* **2005**, *127* (33), 11548–11549.
(14) Mei, X.; Wolf, C. *J. Am. Chem. Soc.* **2006**, *128* (41), 13326–13327.
(15) Feuster, E. K.; Glass, T. E. *J. Am. Chem. Soc.* **2003**, *125* (52), 16174–16175.
(16) Thomas, S. W.; Joly, G. D.; Swager, T. M. *Chem. Rev.* **2007**, *107* (4), 1339–1386.
(17) Jenekhe, S. A.; Osaheni, J. A. *Science* **1994**, *265* (5173), 765–8.
(18) Langhals, H.; Krotz, O.; Polborn, K.; Mayer, P. *Angew. Chem., Int. Ed.* **2005**, *44* (16), 2427–2428.
(19) Samuel, I. D. W.; Turnbull, G. A. *Chem. Rev.* **2007**, *107* (4), 1272–1295.
(20) Naddo, T.; Che, Y.; Zhang, W.; Balakrishnan, K.; Yang, X.; Yen, M.; Zhao, J.; Moore, J. S.; Zang, L. *J. Am. Chem. Soc.* **2007**, *129* (22), 6978–6979.
(21) Newman, C. R.; Frisbie, C. D.; da Silva Filho, D. A.; Bredas, J.-L.; Ewbank, P. C.; Mann, K. R. *Chem. Mater.* **2004**, *16* (23), 4436–4451.
(22) Zang, L.; Che, Y.; Moore, J. S. *Acc. Chem. Soc.* **2008**, DOI: 10.1021/ar8000302, in press.
(23) Wurthner, F. *Chem. Commun.* **2004**, (14), 1564–79.
(24) Langhals, H. *Helv. Chim. Acta* **2005**, *88* (6), 1309–1343.
(25) Schenning, A. P. H. J.; Meijer, E. W. *Chem. Commun.* **2005**, (26), 3245–3258.
(26) Hoeben, F. J. M.; Jonkheijm, P.; Meijer, E. W.; Schenning, A. P. H. J. *Chem. Rev.* **2005**, *105* (4), 1491–1546.
(27) Che, Y.; Datar, A.; Balakrishnan, K.; Zang, L. *J. Am. Chem. Soc.* **2007**, *129* (23), 7234–7235.
(28) Balakrishnan, K.; Datar, A.; Oitker, R.; Chen, H.; Zuo, J.; Zang, L. *J. Am. Chem. Soc.* **2005**, *127*, 10496–10497.
(29) Balakrishnan, K.; Datar, A.; Naddo, T.; Huang, J.; Oitker, R.; Yen, M.; Zhao, J.; Zang, L. *J. Am. Chem. Soc.* **2006**, *128*, 7390–7398.
(30) Ahrens, M. J.; Sinks, L. E.; Rybtchinski, B.; Liu, W.; Jones, B. A.; Giaimo, J. M.; Gusev, A. V.; Goshe, A. J.; Tiede, D. M.; Wasielewski, M. R. *J. Am. Chem. Soc.* **2004**, *126* (26), 8284–8294.
(31) Paramonov, S. E.; Jun, H. W.; Hartgerink, J. D. *J. Am. Chem. Soc.* **2006**, *128* (22), 7291–7298.
(32) Hartgerink, J. D.; Beniash, E.; Stupp, S. I. *Science* **2001**, *294*, 1684–8.
(33) Genson, K. L.; Holzmueller, J.; Ornatska, M.; Yoo, Y. S.; Par, M. H.; Lee, M.; Tsukruk, V. V. *Nano Lett.* **2006**, *6* (3), 435–440.
(34) Zubarev, E. R.; Sone, E. D.; Stupp, S. I. *Chem. Eur. J.* **2006**, *12* (28), 7313–7327.
(35) Beck, J. S.; VartUli, J. C.; Roth, W. J.; Leonowicz, M. E.; Kresge, C. T.; Schmitt, K. D.; Chu, C. T.-W.; Olson, D. H.; Sheppard, E. W.; McCullen, S. B.; Higgins, J. B.; Schlenke, J. L. *J. Am. Chem. Soc.* **1992**, *114*, 10834.
(36) Balakrishnan, K.; Datar, A.; Zhang, W.; Yang, X.; Naddo, T.; Huang, J.; Zuo, J.; Yen, M.; Moore, J. S.; Zang, L. *J. Am. Chem. Soc.* **2006**, *128*, 6576–6577.
(37) Rybtchinski, B.; Sinks, L. E.; Wasielewski, M. R. *J. Am. Chem. Soc.* **2004**, *126*, 12268–12269.
(38) Hill, J. P.; Jin, W.; Kosaka, A.; Fukushima, T.; Ichihara, H.; Shimomura, T.; Ito, K.; Hashizume, T.; Ishii, N.; Aida, T. *Science* **2004**, *304* (5676), 1481–1483.
(39) Yamamoto, Y.; Fukushima, T.; Suna, Y.; Ishii, N.; Saeki, A.; Seki, S.; Tagawa, S.; Taniguchi, M.; Kawai, T.; Aida, T. *Science (Washington, DC, U.S.)* **2006**, *314* (5806), 1761–1764.
(40) Zhang, X.; Chen, Z.; Wurthner, F. *J. Am. Chem. Soc.* **2007**, *129* (16), 4886–4887.
(41) Zang, L.; Liu, R.; Holman, M. W.; Nguyen, K. T.; Adams, D. M. *J. Am. Chem. Soc.* **2002**, *124* (36), 10640–10641.
(42) Cumming, C. J.; Aker, C.; Fisher, M.; Fox, M.; Grone, M. J. l.; Reust, D.; Rockley, M. G.; Swager, T. M.; Towers, E.; Williams, V. *IEEE Trans. Geosci. Remote Sensing* **2001**, *39*, 1119–1128.

NL080761G